

# A New Class of Pyrochlore Solid Solution Formed by Chemical Intercalation of Oxygen

James B. Thomson, A. Robert Armstrong, and Peter G. Bruce\*

Contribution from the School of Chemistry, University of St. Andrews,  
North Haugh, St. Andrews, Fife KY16 9ST, Scotland

Received April 11, 1996. Revised Manuscript Received July 8, 1996<sup>⊗</sup>

**Abstract:** Oxygen intercalation into a pyrochlore at room temperature is reported. A simple chemical route was employed. Previously only perovskite or a few closely related phase have demonstrated an ability to act as hosts for such intercalation. The specific system studied was the interstitial solid solution  $\text{Ce}_2\text{Zr}_2\text{O}_{7+x}$  ( $0 \leq x \leq 0.36$ ). Neutron diffraction reveals that interstitial oxygen enters the tetrahedral 8b sites (space group  $Fd\bar{3}m$ ), which are empty in stoichiometric pyrochlore, but displacement of existing oxygen from the tetrahedral 8a sites also occurs. The lattice contracts on intercalation due to oxidation of  $\text{Ce}^{3+}$ . The changes in structure and the diffusion pathways for oxygen are discussed.

## Introduction

Intercalation may be defined as the process of inserting a guest atom or molecule into a host solid or removing such species from a solid without inducing a major disruption of the host structure. Several excellent reviews on this topic are available.<sup>1–3</sup> Intercalation provides the ability to vary the composition and structure of solids in a controlled manner often at temperatures far below those usually employed in solid state synthesis. As a result new metastable structures may be formed which differ from those available from high-temperature solid state reaction. For example, it has recently been reported that lithium can be removed at room temperature from the layered compound  $\text{LiCoO}_2$ , yielding the new compound  $\text{CoO}_2$  which contains exclusively the relatively unstable  $\text{Co}^{4+}$  ion.<sup>4</sup> Furthermore such metastable intercalation compounds often exhibit unusual but desirable electrical, magnetic, and optical properties. Intercalation plays an important role in the area of microporous solids with regard to their catalytic properties. In addition, its importance in the field of rechargeable lithium batteries, where such compounds act as electrodes, has been recognized.<sup>3</sup> The development of lithium intercalation electrodes has resulted in the successful realization of this technology.<sup>5–9</sup>

Intercalation of cations and molecular species has been extensively studied in recent years.<sup>1–3,10–13</sup> In contrast, the investigation of anion intercalation has received somewhat less

attention. The lack of studies aimed at a better understanding of oxygen intercalation, in particular, is surprising given the importance of oxide chemistry in general. An example is the importance, of oxygen stoichiometry in high-temperature superconductors. Pouchard *et al.* have reported the insertion of oxygen into the brownmillerite  $\text{Sr}_2\text{Fe}_2\text{O}_5$ , forming the perovskite  $\text{SrFeO}_3$ .<sup>14</sup> Oxygen intercalation into solids with the  $\text{K}_2\text{NiF}_4$  structure type, specifically  $\text{La}_2\text{CuO}_4$  and  $\text{La}_2\text{NiO}_4$ , has been reported by Pouchard, Schöllhorn, Jacobson, Radaelli, and their co-workers.<sup>15–18</sup> To date, the range of structures acting as hosts for oxygen intercalation appears to be limited to the perovskite and related  $\text{K}_2\text{NiF}_4$  structure types.

Pyrochlore oxides possess the general formula  $\text{A}_2\text{B}_2\text{O}_7$ . Their structure may be described as an ordered cubic close-packed array of cations with the A and B cations located respectively at the 16c and 16d sites in the space group  $Fd\bar{3}m$ . Oxide ions occupy  $7/8$  of the tetrahedral sites between the cations. The oxide subarray is divided into two sets of tetrahedral sites. Six of the seven oxide ions are located at the 48f position with the remaining oxide ion residing on an 8a site. Two interstitial sites are available for oxygen. One is a tetrahedral site designated 8b, whereas the other is an octahedral site designated 32e. The pyrochlore structure is related to that of fluorite,  $\text{AO}_2$ , but with ordered cations and ordered vacancies in  $1/8$  of the tetrahedral anion sites. Pyrochlore oxides can exhibit a range of important and interesting behavior. The electrical properties of the pyrochlores can vary from insulating through semiconducting to metallic, and the insulating pyrochlores can demonstrate piezoelectric and ferroelectric behavior. Pyrochlore oxides can also sustain significant oxide ion conductivity even when

\* Author to whom correspondence should be addressed.

⊗ Abstract published in *Advance ACS Abstracts*, October 15, 1996.

(1) *Intercalation Chemistry*, Jacobson, A. J., Whittingham, M. S., Eds.; Academic Press Inc.: New York, 1982.

(2) O'Hare, D. In *Inorganic Materials*; Bruce, D. W., O'Hare, D., Eds.; John Wiley: New York, 1995.

(3) Whittingham, M. S. *Prog. Solid State Chem.* **1978**, *12*, 41.

(4) Amatucci, G. G.; Tarascon, J. M.; Klein, L. C. *J. Electrochem. Soc.* **1996**, *143*, 1114.

(5) Nagaura, T. 3rd International Battery Seminar, Deerfield Beach, FL, 1990.

(6) Mizushima, K.; Jones, P. C.; Wiseman, P. J., Goodenough, J. B. *Mater. Res. Bull.* **1980**, *17*, 785.

(7) Thackeray, M. M.; David, W. I. F.; Bruce, P. G.; Goodenough, J. B. *Mater. Res. Bull.* **1983**, *18*, 461.

(8) Armstrong, A. R.; Bruce, P. G. *Nature* **1996**, *381*, 499.

(9) Tarascon, J. M.; Schmutz, C.; Gozdz, A. S.; Warren, P. C.; Shokoohi, F. K. *Mater. Res. Soc. Symp. Proc.* **1995**, *369*, 595.

(10) Bruce, P. G.; Nowinski, J.; Gibson, V. C.; Hauptman, Z. V.; Shaw, A. J. *Solid State Chem.* **1990**, *89*, 202–207.

(11) Johnson, J. W.; Jacobson, A. J.; Rich, S. M.; Brody, J. F. *J. Am. Chem. Soc.* **1981**, *103*, 5246.

(12) Dickens, P. G.; Chippindale, A. M.; Hibble, S. J. *Solid State Ionics* **1989**, *34*, 79.

(13) Dickens, P. G.; Hawke, S. V.; Weller, M. T. *Mater. Res. Bull.* **1984**, *19*, 543.

(14) Grenier, J.-C.; Wattiaux, A.; Doumerc, J.-P.; Dordor, P.; Fournes, L.; Chaminade, J.-P.; Pouchard, M. *J. Solid State Chem.* **1992**, *96*, 20.

(15) Wattiaux, A.; Park, J. C.; Grenier, J.-C.; Pouchard, M. *C. R. Acad. Sci.* **1990**, *310*, 1047.

(16) Rudolf, P.; Schöllhorn, R. *J. Chem. Soc., Chem. Commun.* **1992**, 1158.

(17) Bhavaragu, S.; Di Carlo, J. F.; Scarfe, D. P.; Jacobson, A. J. Proceedings of the 10th International Conference on Solid State Ionics, Singapore, 1996, in press.

(18) Radaelli, P. G.; Jorgensen, J. D.; Schultz, A. J.; Hunter, B. A.; Wagner, J. L.; Chou, F. C.; Johnston, D. C. *Phys. Rev. B* **1993**, *48*, 499.

stoichiometric, e.g.  $\text{Gd}_2\text{Zr}_2\text{O}_7$ ,<sup>19</sup> unlike most other oxide ion conductors for which solid solutions must be formed, such as the doped fluorites, e.g.  $\text{Zr}_{1-x}\text{Ce}_x\text{O}_{2-x}$ .

In this paper we report the chemical intercalation of oxygen at room temperature into a pyrochlore. The specific system studied is based on  $\text{Ce}_2\text{Zr}_2\text{O}_7$ . Whereas vacancy solid solutions with the pyrochlore structure may readily be formed, e.g.  $(\text{Gd}_{2-x}\text{Ca}_x)\text{Zr}_2\text{O}_{7-x}$ , the intercalated pyrochlore  $\text{Ce}_2\text{Zr}_2\text{O}_{7+x}$  represents one of the few interstitial solid solutions based on this structure type. This work opens the way to controlled and precise modification by intercalation of pyrochlore oxides.<sup>20</sup>

## Experimental Section

The host pyrochlore,  $\text{Ce}_2\text{Zr}_2\text{O}_7$ , has been previously prepared by two different routes.<sup>21</sup> One involved the rapid heating and combustion of aqueous solutions of cerium(III) nitrate and zirconium(IV) nitrate with carbohydrazide/urea in the required molar ratio; the second relied on the fusion of appropriate quantities of  $\text{BaCl}_2$ ,  $\text{CeCl}_3$ , and  $\text{BaZrO}_3$  under vacuum at 1000 °C with subsequent leaching of  $\text{BaCl}_2$ . We have devised an alternative method.  $\text{Zr}(\text{OC}_2\text{H}_5)_4$  (Aldrich, 98%) and  $\text{Ce}_2(\text{C}_2\text{O}_4)_3$  (Aldrich, 99.9%) were added in appropriate molar ratios to 250 mL of distilled water, and the mixture was placed in an ultrasonic bath for 2 h followed by vigorous stirring for 48 h. Approximately 200 mL of water was removed by rotary evaporation with the remaining water being taken off by freeze-drying. The resulting powder was placed in an alumina crucible with a lid and transferred to a tube furnace. The sample was heated at 2 deg/min to 250 °C under an atmosphere of 95%  $\text{Ar}/5\%$   $\text{H}_2$ , and this temperature was maintained for 30 min to permit decomposition of the organic material. The temperature was then raised at 10 deg/min to 1300 °C where it was held for 18 h and then cooled to room temperature again at 10 deg/min. The samples were stored in an argon-filled glovebox.

Intercalation was carried out chemically using a 0.5 M solution of sodium hypobromite,  $\text{NaOBr}$ , in distilled water. The powdered  $\text{Ce}_2\text{Zr}_2\text{O}_7$  host was added to a sufficient quantity of this solution to ensure a 5-fold molar excess of the hypobromite. The solution was stirred vigorously to ensure a homogeneous exposure of the crystallites to the solution. Intercalation was carried out under argon and used water which had been previously deoxygenated by bubbling argon through it for 30 min. These procedures were followed in order to avoid oxidation from any source other than the  $\text{NaOBr}$ . The quantity of oxygen in water can vary significantly and could lead to uncontrolled oxidation of the host. After reacting for times ranging from 30 min to 72 h, the product was washed with distilled water and acetone, dried, and then stored in an argon-filled glovebox. Powder X-ray diffraction was carried out by sealing the samples in Lindemann tubes which were then mounted on a Stoe STADI/P powder diffractometer operating in transmission mode and with  $\text{Cu K}\alpha_1$  radiation. Data were collected over the range  $5^\circ < 2\theta < 85^\circ$  in steps of  $0.02^\circ$ .

Time-of-flight powder neutron diffraction data were collected at 298 K on the POLARIS high-intensity, medium-resolution diffractometer at ISIS, Rutherford Appleton Laboratory.<sup>22</sup> Data from the highest resolution backscattering detectors were refined by the Rietveld method using the CCSL suite of programs.<sup>23</sup> Neutron-scattering lengths used were  $\text{Zr} = 0.7160$ ,  $\text{Ce} = 0.4840$ , and  $\text{O} = 0.5803 \times 10^{-12} \text{ cm}^2$ .

## Results and Discussion

Powder X-ray diffraction data collected on the parent  $\text{Ce}_2\text{Zr}_2\text{O}_7$  and samples exposed to the oxidizing agent for increasing

(19) Tuller, H. I.; Kramer, S. Spears, M. A. *High Temperature Electrochemistry*. 14th Riso Symposium, Denmark, 1993; 151.

(20) Thomson, J. B.; Armstrong, A. R.; Bruce, P. G. *J. Chem. Soc., Chem. Commun.* in press.

(21) (a) Casey, J. J.; Katz, L.; Orr, W. C. *J. Am. Chem. Soc.* **1955**, *77*, 2187. (b) Dhas, N. A.; Patil, K. C. *J. Mater. Chem.* **1993**, *3*, 1289.

(22) Smith, R. L.; Hull, S.; Armstrong, A. R. *Mater. Sci. Forum* **1994**, *166–169*, 251.

(23) (a) Matthewman, J. C.; Thompson, P.; Brown, P. J. *J. Appl. Crystallogr.* **1982**, *15*, 167. (b) Brown, P. J.; Matthewman, J. C. Rutherford Appleton Laboratory Report, RAL-87-010; 1987.

(24) Sears, V. F. *Neutron News* **1992**, *3*, (3), 26.

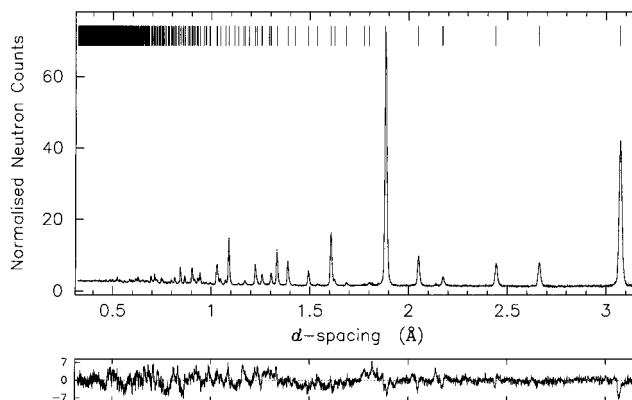


**Figure 1.** Observed (dots) and calculated (solid line) diffraction profiles for  $\text{Ce}_2\text{Zr}_2\text{O}_{7.36}$ . The lower plot shows the difference/esd.

lengths of time exhibited the same diffraction pattern but with a continuous shift in the peak positions indicative of a continuous range of solid solution. In order to explore the structural changes accompanying the reaction, in particular to verify that oxygen intercalation had taken place and if so to determine its extent and the positions occupied by the oxide ions, neutron diffraction was carried out. Fifteen samples were studied which had been exposed to the sodium hypobromite solution for different times, as well as the parent cerium zirconate itself.

In all cases the neutron powder diffraction patterns could be indexed in the space group ( $Fd\bar{3}m$ , No. 227) appropriate for the pyrochlore structure. A stoichiometric pyrochlore structural model ( $\text{Ce}_2\text{Zr}_2\text{O}_7$ ) was used as a starting point for the refinements. A similar procedure was adopted for refining the structures of all the compositions. Initially the Ce and Zr ions were placed on the 16c and 16d sites and their occupancies were allowed to vary; however these were refined to unity within 2 esds. Attempts to refine a model in which the cerium and zirconium ions were allowed to exchange between the 16c and 16d sites indicated that cerium remained exclusively on the 16c and zirconium on the 16d sites, thereby demonstrating that there is no antisite disorder between the A and B sites although it is known to be a common feature of many pyrochlore oxides. The refinement also explored the possibility of oxide ion vacancies on the tetrahedral 48f sites; however, it proved impossible to vary oxygen occupancy on this site, with a value of unity being consistently obtained within 2 esds. Occupancy of the two interstitial sites available for oxide ions in the pyrochlore structure, tetrahedral 8b and octahedral 32e, was explored. All attempts to refine an oxygen occupancy in the latter site failed, indicating that this site is not involved in the formation of the interstitial solid solutions. Oxide ions were, however, located in the 8b site. In the final refinements for each composition, the occupancy of the Ce and Zr ions was fixed at unity on the A and B sites, respectively, as was the occupancy of oxygen on the 48f sites. A fitted powder diffraction profile for the composition with the maximum oxygen content in the solid solution series is shown in Figure 1, and the associated refined crystallographic data are presented in Table 1. This particular refinement yielded an  $R_{\text{wp}}$  of 2.96%,  $R_e$  of 1.39%, and  $\chi^2$  of 4.53. A model of the structure highlighting the oxygen positions is shown in Figure 2. The fit is typical of those obtained for all the compositions studied. In summary, the structure consists of an ordered cubic close-packed array of Ce and Zr with O in three sets of tetrahedral sites, two of which are only partially occupied. The refined oxygen occupancies of the tetrahedral 8a and 8b sites are presented in Figure 3 where they are plotted against the total oxygen content determined by addition of these

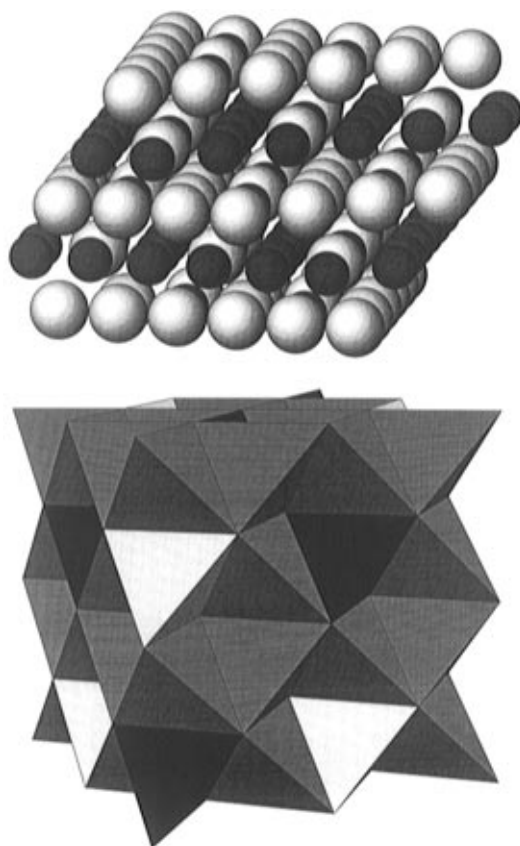
**Table 1.** Structural and Thermal Parameters for  $\text{Ce}_2\text{Zr}_2\text{O}_{7.36}$ 

a. Structural Parameters for $\text{Ce}_2\text{Zr}_2\text{O}_{7.36}^a$					
atom	Wyckoff symbol	$x/a$	$y/a$	$z/a$	fractional occupancy
Ce	16c	0.0	0.0	0.0	1
Zr	16d	0.5	0.5	0.5	1
O1	48f	0.40586 (11)	0.125	0.125	1
O2	8a	0.125	0.125	0.125	1.007 (17)
O3	8b	0.375	0.375	0.375	0.357 (12)

b. Thermal Parameters ( $\text{\AA}^2$ ) for $\text{Ce}_2\text{Zr}_2\text{O}_{7.36}$						
atom	$B_{11}$	$B_{22}$	$B_{33}$	$B_{23}$	$B_{13}$	$B_{12}$
Ce	0.42 (3)	0.42	0.42	-0.08 (3)	-0.08	-0.08
Zr	0.68 (2)	0.68	0.68	0.32 (3)	0.32	0.32
O1	2.54 (5)	0.52 (2)	0.52 (2)	-0.28 (3)		
O2	0.92 (5)					
O3	0.92 (5)					

<sup>a</sup> Cubic, space group  $Fd\bar{3}m$ ;  $a = 10.6440(1)$   $\text{\AA}$ .



**Figure 2.** (Top) Structure of  $\text{Ce}_2\text{Zr}_2\text{O}_{7+x}$  showing the close-packed array of Ce (pale circles) and Zr (dark circles). (Bottom) Structure of  $\text{Ce}_2\text{Zr}_2\text{O}_{7+x}$  emphasizing the tetrahedrally coordinated oxygen sites. An oxygen is at the center of each tetrahedron with four cations at the vertices. Pale tetrahedra represent 8a oxygen sites coordinated by four Ce. Dark tetrahedra represent 8b oxygen sites coordinated by four Zr. Medium tetrahedra represent oxygen on 48f sites coordinated by two Ce and two Zr.

occupancies. These data reveal a most interesting effect: contrary to initial expectation, the intercalated oxygen does not reside on the tetrahedral 8b sites with the original oxygen subarray remaining intact; instead, as the guest oxygen content increases, the occupancy of the 8b site increases to a greater extent, the additional oxygen arising from displacement of oxide ions from the tetrahedral 8a site. This continued up to an oxygen content of  $x = 0.2$  in  $\text{Ce}_2\text{Zr}_2\text{O}_{7+x}$ . Above this composition, occupancy of the 8a site rises again as that of the 8b site appears to saturate. Evidently the mechanism of

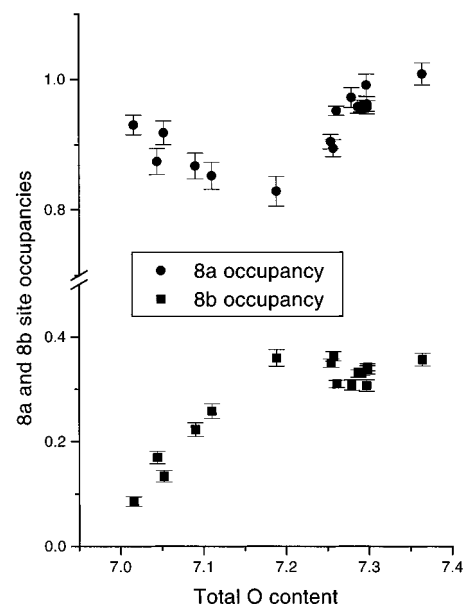


**Figure 3.** Variation in the refined occupancies of the tetrahedral 8a and 8b sites in  $\text{Ce}_2\text{Zr}_2\text{O}_{7+x}$  as a function of total refined oxygen content.

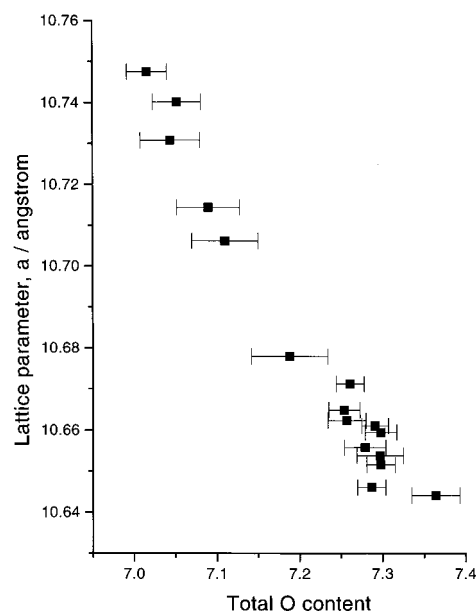


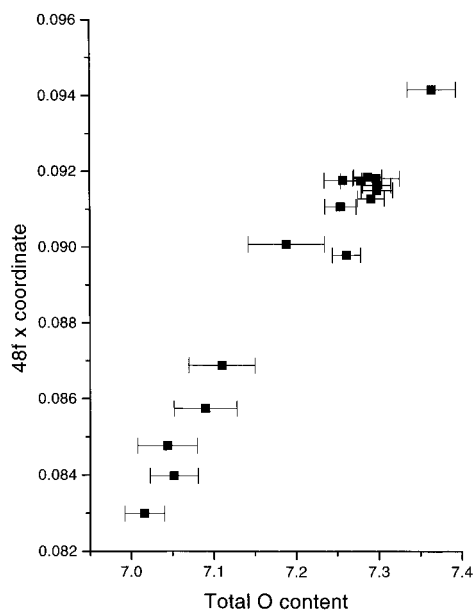
**Figure 4.** Variation in the lattice parameter of  $\text{Ce}_2\text{Zr}_2\text{O}_{7+x}$  as a function of total refined oxygen content.

interstitial solid solution formation for this pyrochlore oxide is not simple and involves disruption of the oxygen subarray in the host compound, but only on the 8a sites. It should be noted that even the stoichiometric parent material,  $\text{Ce}_2\text{Zr}_2\text{O}_7$ , exhibits a smaller but finite displacement of oxygen (7%) from the 8a to the 8b site. The maximum oxygen content,  $x = 0.36$  appears to be set by the intrinsic strength of the  $\text{OBr}^-$  oxidizing agent, since in principle a value of 1 could be obtained. Extending the reaction time or using more concentrated solutions of  $\text{NaOBr}$  did not yield higher oxygen contents.

Further confirmation concerning the nonideal nature of the solid solution is obtained by examining Figure 4, which presents the variation of lattice parameter with the total oxygen content. As the degree of oxygen intercalation is increased, the lattice parameter continuously contracts. However, that contraction seems not to be linear; instead it appears to exhibit a negative deviation from Vegard's law. The fact that contraction rather than expansion occurs upon intercalation demonstrates that the

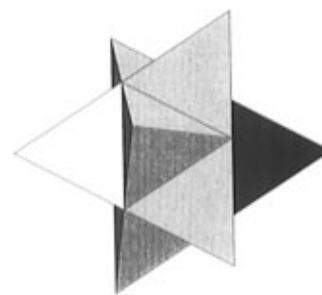
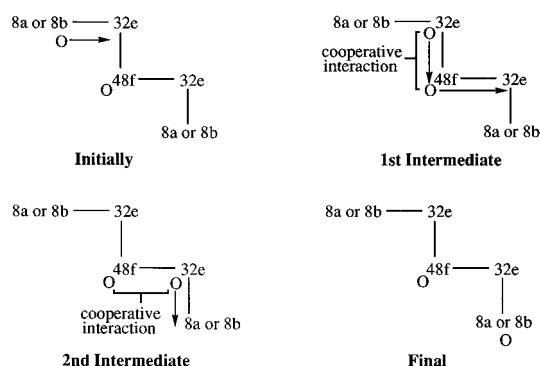
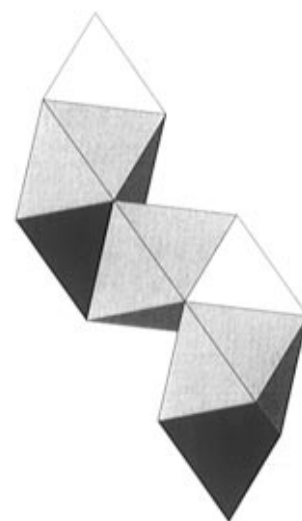
**Table 2.** Effective Ionic Radii (Å) for Ce and Zr for Coordination Numbers 6, 7, and 8<sup>25</sup>

element	6-coordinate	7-coordinate	8-coordinate
Ce <sup>3+</sup>	1.01	1.07	1.143
Ce <sup>4+</sup>	0.87		0.97
Zr <sup>4+</sup>	0.72	0.78	0.84

**Figure 5.** Variation in 48f site positional parameter in Ce<sub>2</sub>Zr<sub>2</sub>O<sub>7+x</sub> as a function of total refined oxygen content.

effect of oxidizing two Ce<sup>3+</sup> ions to the smaller Ce<sup>4+</sup> ions, Table 2, is greater than the influence of the additional oxide ion.

Two important questions arise from the above structural data on the pyrochlore solid solutions concerning the mechanism of intercalation, i.e. solid solution formation. The first question is, why are the 8a site oxide ions displaced to the 8b positions? The second question is, what are the diffusion pathways followed by the oxide ions on insertion into the parent Ce<sub>2</sub>Zr<sub>2</sub>O<sub>7</sub>? Let us begin by addressing the first of these questions. In order to understand the displacement of oxide ions, it is important first to recall the local coordination around the ions in the pyrochlore structure. Although the parent Ce<sub>2</sub>Zr<sub>2</sub>O<sub>7</sub> exhibits a small displacement of oxide ions, it is more convenient to describe the coordination in terms of an ideal pyrochlore structure. In this case the Ce<sup>3+</sup> ions are surrounded by eight oxide ions, six of which are located at 48f positions while the remaining two are oxide ions on 8a sites. The Zr<sup>4+</sup> ions are octahedrally coordinated by oxide ions belonging exclusively to the 48f sites; two vacant 8b positions also coordinate to the zirconium ions. Considering now the coordination around the anions, each oxide ion in an 8a site is surrounded tetrahedrally by four Ce<sup>3+</sup> ions. The 48f sites are tetrahedrally coordinated by two Ce<sup>3+</sup> and two Zr<sup>4+</sup> ions, and finally the empty 8b sites are coordinated tetrahedrally by four Zr<sup>4+</sup> ions. The vacant interstitial octahedral 32e positions are surrounded by three Ce<sup>3+</sup> and three Zr<sup>4+</sup> ions. Up to an oxygen stoichiometry of  $x = 0.2$ , the guest oxide ions are inserted into the tetrahedral 8b sites rather than the octahedral 32e positions. Comparing the Zr–O bond lengths for oxygen located in 8b (2.305 Å) and 32e positions (2.662 Å), it is evident that the bond length in the latter case is larger than that which is typical for such bonds (these range from 2.0 to 2.3 Å in ZrO<sub>2</sub>). It is clear, therefore, that the size of the oxide ion more closely matches the

**Figure 6.** Pyrochlore structure illustrating one 8a site (pale tetrahedron) and one 8b site (dark tetrahedron) linked by a ring of six 48f sites (medium tetrahedra). One 48f site is eclipsed.**Figure 7.** (Top) Pyrochlore structure illustrating linkage of tetrahedral 8a (pale) and 8b sites (dark) via octahedral 32 site. (Bottom) Schematic illustration of the cooperative conduction mechanism in Ce<sub>2</sub>Zr<sub>2</sub>O<sub>7+x</sub>. The movement of oxide ions is represented at four stages which together constitute a complete migration step. The sequence 8a or 8b–32e–48f–32e–8a or 8b corresponds to the face-sharing sites through which the oxide ions migrate. Oxygen positions are represented by O, and their direction of movement is represented by arrows.

tetrahedral site, and it is for this reason that the guest oxide ions occupy the 8b position. Furthermore, it is known that Zr prefers a coordination number of 7 in an oxide environment. This is evident if one considers ZrO<sub>2</sub>, which only adopts the cubic fluorite structure at high temperatures; more modest temperatures permit a distortion of the structure to yield 7-coordinate zirconium. Each oxide ion in an 8b site in the pyrochlore structure will coordinate four zirconium ions. Provided neighboring 8b sites are not occupied (and this would only occur above an occupancy of 0.5 which is not reached in this system), an average coordination number of between 6 and 7 will be obtained for the zirconium ions. The occupancy of an oxide ion in a 32e position would coordinate only three

(25) Shannon, R. D. *Acta Crystallogr., Sect. A* 1976, 32, 751.

zirconium ions. Having established the preference of an oxide ion for the 8b positions, it is important to recall that the intercalation of each oxide ion results in the oxidation of two  $\text{Ce}^{3+}$  ions to two  $\text{Ce}^{4+}$  ions. Whereas in the parent  $\text{Ce}_2\text{Zr}_2\text{O}_7$  pyrochlore, the ionic radii of the  $\text{Ce}^{3+}$  and  $\text{Zr}^{4+}$  ions in their 8 and 6 coordinate sites, respectively are 1.143 and 0.72 Å, yielding a ratio of 1.59, which is comfortably within the range 1.46–1.8 that can be tolerated by the pyrochlore structure, oxidation of  $\text{Ce}^{3+}$  to  $\text{Ce}^{4+}$  results in an ionic radius of 0.97 Å, and  $\text{Zr}^{4+}$ , in a 7-coordinate oxygen site, will possess an ionic radius of 0.78 Å, Table 2. As a result of the change in ionic radii, different oxygen coordinations around the ions are no longer tolerable; hence oxide ions will be displaced from the 8a to the 8b sites. In other words, as the radii of the ions on the A and B sites converge, the oxide ion distribution more closely approaches that in the fluorite structure. In addition to these changes, the position parameter of the oxide ions in the 48f sites also varies with the total oxygen content, Figure 5. This corresponds to a shift of the oxide ions away from the empty 8b site and toward the center of the 48f site. One 8a, one 8b, and six 48f sites are shown in Figure 6. The displacement of the oxide ions in the 48f positions involves a slight shift of the “ring” of oxide ion so that these ions approach a position equidistant between the 8a and 8b sites. Again this emphasizes the move toward an oxide distribution which more closely approximates that of the fluorite structure. For an oxide ion content greater than 7.2, further intercalation does not result in a significant increase in occupancy of the 8b sites, but instead we see a rise in occupancy of the 8a sites. Although diffraction data yield only average occupancies, it is likely that the oxide ions redistribute themselves so as to satisfy, as far as is possible, the local coordination requirements of the ions. For example, it is likely that oxide ions are displaced from 8a sites surrounding cerium ions which are oxidized to the 4+ oxidation state. However, conclusions the local structure would require investigation by other techniques such as diffuse scattering or oxygen NMR.

The second question raised above concerns the pathways for oxide ion diffusion through the cerium zirconate structure;

examination of the neutron data can assist elucidation of this. Figure 7a illustrates the fact that each tetrahedral 8a and 8b site is linked by an intervening 32e octahedral position, involving the sharing of two opposite faces of the octahedron, one with each of the tetrahedral sites. Each 8a and 8b site shares all four faces with 32e octahedra, thus forming a continuous network of face-sharing octahedra and tetrahedra in three dimensions throughout the structure. The oxide ions which partially occupy the 8a and 8b sites may therefore migrate between these sites through the empty 32 positions. The 8a and 8b sites do not share faces with themselves or with each other. An alternative mechanism involving cooperative motion is also possible. In this case an oxide ion from either an 8a or an 8b site moves into a 32e position where it displaces an oxide ion from one of the 48f positions into a second 32e site; each 48f site shares all four of its faces with a 32e site. The resulting empty 48f site would subsequently be occupied by the oxide ion which originated in the 8a or 8b site. Motion of oxide ions involving this second pathway would constitute an interstitialcy mechanism since it involves displacement of ions which fully occupy a set of sites and that, therefore, do not give rise to diffusion in themselves but are merely part of a cooperative conduction mechanism. This mechanism is shown in Figure 7b. The nature of electronic transport, which is also part of the intercalation process, is not known in detail but is expected to be similar to that in the nonstoichiometric fluorite  $\text{CeO}_{2-x}$ , which is related structurally to the pyrochlore. This involves electron hopping between localized sites on the Ce ions.

Having demonstrated that oxygen can be intercalated into  $\text{Ce}_2\text{Zr}_2\text{O}_7$  to yield an interstitial solid solution, it may be anticipated that this process can be carried out with other pyrochlore oxides, leading to new interstitial pyrochlore solid solutions.

**Acknowledgment.** P.G.B. is indebted to the EPSRC and the Leverhulme Trust for financial support. The authors are grateful to the ISIS staff, in particular Dr. S. Hull, for their assistance.

JA961202R